Neural Comput & Applic (2010) 19:565–571
DOI 10.1007/s00521-009-0319-2

ORIGINAL ARTICLE

Limit cycle prediction of a neurocontrol vehicle system based on gain-phase margin analysis

Jau-Woei Perng · Li-Shan Ma · Bing-Fei Wu

Received: 21 March 2009 / Accepted: 15 October 2009 / Published online: 31 October 2009
© Springer-Verlag London Limited 2009

Abstract Based on some useful frequency domain methods, this paper proposes a systematic procedure to address the limit cycle prediction of a neural vehicle control system with adjustable parameters. A simple neurocontroller can be linearized by using describing function method firstly. According to the classical method of parameter plane, the stability of linearized system with adjustable parameters is then considered. In addition, gain margin and phase margin for limit cycle generation are also analyzed by adding a gain-phase margin tester into open loop system. Computer simulations show the efficiency of this approach.

Keywords Neural network · Describing functions · Gain-phase margin · Vehicle

1 Introduction

The traditional method of analyzing the amplitude and frequency of a limit cycle is to linearize the nonlinear elements according to the describing function method [1–9]. Recently, this method has been extended to analyze the stability of fuzzy [10, 11] and neural systems [12, 13]. Uncertain parameters in a linear control system can be robustly analyzed by the parameter plane method or the parameter space method [14–17]. A designer must carefully consider the range of safe operation of a system since varying parameters and phase lag always impact practical control systems. Gain margin (GM) and phase margin (PM) are two important specifications in the analysis and design of practical control systems. Methods of analyzing the gain-phase margin of linear control systems [18–20] and nonlinear systems [21–24] with adjustable parameters have been developed.

This work describes a systematic strategy for analyzing the limit cycles of a neural vehicle control system [9] with adjustable parameters. The vehicle model is a single track model from steering angle to yaw rate. A simple method is then presented to evaluate the gain-phase margins for limit cycle prediction after a gain-phase margin tester is added to the forward open loop of a linearized vehicle control system. After doing this, the relationship between the amplitude of limit cycles and stability margins can be easily figured out.

J.-W. Perng (✉)
Department of Mechanical and Electro-Mechanical Engineering, National Sun Yat-sen University, 70, Lienhai Road, Kaohsiung 80424, Taiwan, ROC
e-mail: jwperng@faculty.nsysu.edu.tw

L.-S. Ma
Department of Electronic Engineering, Chienkuo Technology University, No. 1, Chieh Shou N. Rd, Changhua City, Taiwan, ROC

L.-S. Ma · B.-F. Wu
Institute of Electrical Control Engineering, National Chiao Tung University, No. 1001, Ta Hsueh Road, Hsinchu 300, Taiwan, ROC

2 Basic approach

In this section, some useful frequency domain approaches including parameter plane, gain-phase margin tester and describing function of neurocontroller are considered for limit cycle prediction of vehicle control systems.

2.1 Parameter plane method

A general linearized system shown in Fig. 1 with multiple nonlinear elements is considered, where $G(s, N_{1R}, N_{1I},$

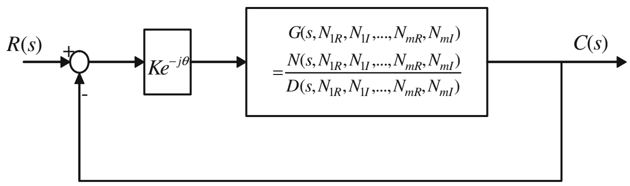

Fig. 1 Block diagram of a general linearized nonlinear control system

$\ldots, N_{mR}, N_{mI})$ is the open loop transfer function. $N_{1R}, \ldots, N_{mR}$ and $N_{1I}, \ldots, N_{mI}$ are real parts and imaginary parts of the describing function (N_i) of $n_1, n_2, \ldots, n_m$, respectively, which can be expressed as the following equation [2, 3]

$$N_i(A,\omega) = N_{iR}(A,\omega) + jN_{iI}(A,\omega), \quad i = 1,\ldots,m, \tag{1}$$

where A and ω are the amplitude and frequency of sinusoidal input to one of the nonlinearities.

The characteristic equation of this equivalent linear system can be expressed as

$$\begin{aligned} &1 + Ke^{-j\theta}G(s, N_{1R}, N_{1I}, \ldots, N_{mR}, \ldots, N_{mI}) \\ &= 1 + Ke^{-j\theta}\frac{N(s, N_{1R}, N_{1I}, \ldots, N_{mR}, \ldots, N_{mI})}{D(s, N_{1R}, N_{1I}, \ldots, N_{mR}, \ldots, N_{mI})} = 0, \end{aligned} \tag{2}$$

which is equivalent to

$$\begin{aligned} f(s) \triangleq\; & D(s, N_{1R}, N_{1I}, \ldots, N_{mR}, \ldots, N_{mI}) \\ & + Ke^{-j\theta}N(s, N_{1R}, N_{1I}, \ldots, N_{mR}, \ldots, N_{mI}) = 0 \end{aligned} \tag{3}$$

Let $s = j\omega$, one has

$$f(j\omega) = f(\alpha, \beta, \gamma, \ldots, K, \theta, j\omega) = 0, \tag{4}$$

where $\alpha, \beta, \gamma, \ldots$ are variables which consist of the items (N_{iR}, N_{iI}) of describing functions and/or adjustable parameters of the linear portion of the system. Notice that the designer can define these variables arbitrarily in order to analyze the effect of system parameters. When only two parameters α and β are chosen to concern, (4) is arranged as the following equation

$$f(j\omega) = f(\alpha, \beta, \gamma, \ldots, K, \theta, j\omega) = X\cdot\alpha + Y\cdot\beta + Z = 0 \tag{5}$$

where X, Y and Z are functions of $\gamma, \ldots, K, \theta$ and $j\omega$. Let Eq. (5) be partitioned into two stability equations with real part (f_R) and imaginary part (f_I) and written in the following [14, 15]

$$f_R(\alpha, \beta, \gamma, \ldots, K, \theta, \omega) = X_1\cdot\alpha + Y_1\cdot\beta + Z_1 = 0 \tag{6}$$

and

$$f_I(\alpha, \beta, \gamma, \ldots, K, \theta, \omega) = X_2\cdot\alpha + Y_2\cdot\beta + Z_2 = 0 \tag{7}$$

where X_1, Y_1, Z_1 and X_2, Y_2, Z_2 are real and imaginary parts of X, Y and Z. Therefore, α and β are solved from linear functions of Eqs. (6) and (7), one has

$$\alpha = \frac{Y_1\cdot Z_2 - Y_2\cdot Z_1}{\Delta} \tag{8}$$

and

$$\beta = \frac{Z_1\cdot X_2 - Z_2\cdot X_1}{\Delta}, \tag{9}$$

where $\Delta = X_1\cdot Y_2 - X_2\cdot Y_1$. Note that if Eqs. (6) and (7) are not linear, but independent with α and β, they can be solved theoretically.

2.2 Gain-phase margin analysis

Let $\theta = 0°$; Eq. (4) is rearranged as follows.

$$f(j\omega) = f(\alpha, \beta, \gamma, \ldots, K, j\omega) = E\cdot K + F = 0. \tag{10}$$

Partitioning Eq. (10) into real and imaginary parts yields

$$f_R(\alpha, \beta, \gamma, \ldots, K, \omega) = E_1\cdot K + F_1 = 0, \tag{11}$$

and

$$f_I(\alpha, \beta, \gamma, \ldots, K, \omega) = E_2\cdot K + F_2 = 0, \tag{12}$$

where E_1, E_2, F_1 and F_2 are functions of $\alpha, \beta, \gamma, \ldots$ and ω. Thus, K can be determined directly from Eqs. (11) and (12), which yield

$$K = \frac{-F_1}{E_1} \triangleq K' \tag{13}$$

and,

$$K = \frac{-F_2}{E_2} \triangleq K''. \tag{14}$$

If $K' = K'' = K_i$ for $A = A_i$, the values of A_i and K_i related to ω_i can be found by varying A from 0 to ∞. For many values of ω, a set (GM) of desired values of A and K can be obtained. Alternatively, let $K = 0$ dB; Eq. (4) is rearranged as follows.

$$f(j\omega) = f(\alpha, \beta, \gamma, \ldots, \theta, j\omega) = U\cdot\cos\theta + V\cdot\sin\theta + W = 0. \tag{15}$$

Also partitioning Eq. (15) into real and imaginary parts yields

$$f_R(\alpha, \beta, \gamma, \ldots, \theta, \omega) = U_1\cdot\cos\theta + V_1\cdot\sin\theta + W_1 = 0 \tag{16}$$

and

$$f_I(\alpha, \beta, \gamma, \ldots, \theta, \omega) = U_2\cdot\cos\theta + V_2\cdot\sin\theta + W_2 = 0, \tag{17}$$

where U_1, V_1, W_1, U_2, V_2 and W_2 are functions of $\alpha, \beta, \gamma, \ldots,$ and ω. Hence, θ can be determined directly from Eqs. (16) and (17), which yield

$$\theta = \cos^{-1}\left(\frac{V_1\cdot W_2 - V_2\cdot W_1}{U_1\cdot V_2 - U_2\cdot V_1}\right) \triangleq \theta' \tag{18}$$

and

$$\theta = \sin^{-1}\left(\frac{U_1\cdot W_2 - U_2\cdot W_1}{U_1\cdot V_2 - U_2\cdot V_1}\right) \triangleq \theta''. \tag{19}$$

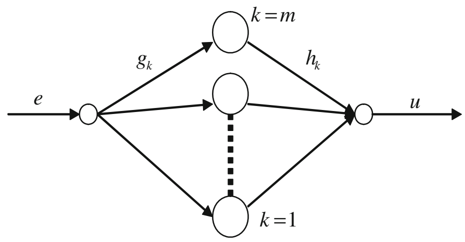

Fig. 2 Static neural network (SNN)

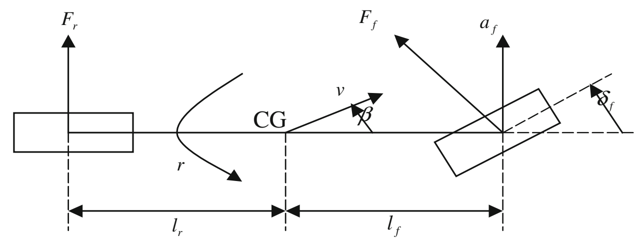

Fig. 3 Single track vehicle model

If $\theta' = \theta'' = \theta_i$ for $A = A_i$, A_i and θ_i related to ω_i can be found by varying A from 0 to ∞. For many values of ω, a set (PM) of desired values for A and θ can be obtained.

2.3 Describing function of a neurocontroller

The static neural network (SNN) shown in Fig. 2 can be used as a controller (neurocontroller). The network structure is 1-m-1 and does not have bias weights [12, 13]. The parameters g_k and h_k are the neural network weights and m is the number of hidden neurons. Based on the stability analysis in [12, 13], the describing function of neurocontroller with sigmoid function *tanh* may be represented as

$$N_1(A) = \sum_{k=1}^{m} g_k \cdot h_k \left\{ 1 - \frac{g_k^2 \cdot A^2}{6} \right\} \tag{20}$$

where A is the amplitude of limit cycle.

3 Vehicle dynamic systems

In the section, the classical linearized single track vehicle model is given first [9]. The vehicle with yaw rate feedback is now considered for design. The transfer function from the input of front deflection angle (δ_f) to the output of yaw rate (r) can be obtained as follows.

Table 1 Vehicle system quantities

F_f, F_r	Lateral wheel force at front and rear wheel
r	Yaw rate
β	Side slip angle at center of gravity (CG)
v	Velocity
a_f	Lateral acceleration
l_f, l_r	Distance from front and rear axis to CG
$l = l_f + l_r$	Wheelbase
δ_f	Front wheel steering angle
m	Mass

The tire force can be expressed as

$$F_f(\alpha_f) = \mu c_{f0} \alpha_f, \quad F_r(\alpha_r) = \mu c_{r0} \alpha_r \tag{22}$$

with the tire cornering stiffnesses c_{f0}, c_{r0}, the road adhesion factor μ and the tire side slip angles

$$\alpha_f = \delta_f - \left(\beta + \frac{l_f}{v} r \right), \alpha_r = -\left(\beta - \frac{l_r}{v} r \right) \tag{23}$$

The state equation of vehicle dynamics with β and r can be represented as

$$\begin{bmatrix} \dot{\beta} \\ \dot{r} \end{bmatrix} = \begin{bmatrix} -\frac{\mu(c_{f0}+c_{r0})}{mv} & -1 + \frac{\mu(c_{r0}l_r - c_{f0}l_f)}{mv^2} \\ \frac{\mu(c_{r0}l_r - c_{f0}l_f)}{m l_f l_r} & -\frac{\mu(c_{f0}l_f^2 + c_{r0}l_r^2)}{m l_f l_r v} \end{bmatrix} \begin{bmatrix} \beta \\ r \end{bmatrix} + \begin{bmatrix} \frac{\mu c_{f0}}{mv} \\ \frac{\mu c_{f0}}{m l_r} \end{bmatrix} \delta_f \tag{24}$$

Hence, the transfer function from δ_f to r is

$$G_{r/\delta_f} = \frac{c_{f0} m l_f \mu v^2 s + c_{f0} c_{r0} l \mu^2 v}{l_f l_r m^2 v^2 s^2 + l(c_{r0} l_r + c_{f0} l_f) m \mu v s + c_{f0} c_{r0} l^2 \mu^2 + (c_{r0} l_r - c_{f0} l_f) m \mu v^2} \tag{25}$$

Figure 3 shows the single track vehicle model, and the related symbols are listed in Table 1. The equations of motion are

$$\begin{bmatrix} mv(\dot{\beta} + r) \\ m l_f l_r \dot{r} \end{bmatrix} = \begin{bmatrix} F_f + F_r \\ F_f l_f - F_r l_r \end{bmatrix} \tag{21}$$

The numerical data in this paper are listed in Table 2. According to the earlier mentioned analysis of a single track vehicle model, the transfer function from the input of front deflection angle δ_f to the output of yaw rate r can be obtained as

$$G_{r/\delta_f}(s,\mu,v) = \frac{(1.382\times10^8\mu v^2 s + 1.415\times10^{10}\mu^2 v)}{6.675\times10^6 v^2 s^2 + 1.08\times10^9 \mu v s + (1.034\times10^7\mu v^2 + 4\times10^{10}\mu^2)} \tag{26}$$

Table 2 Vehicle system parameters

C_{f0}	50,000 N/rad
c_{r0}	100,000 N/rad
m	1,830 kg
l_f	1.51 m
l_r	1.32 m

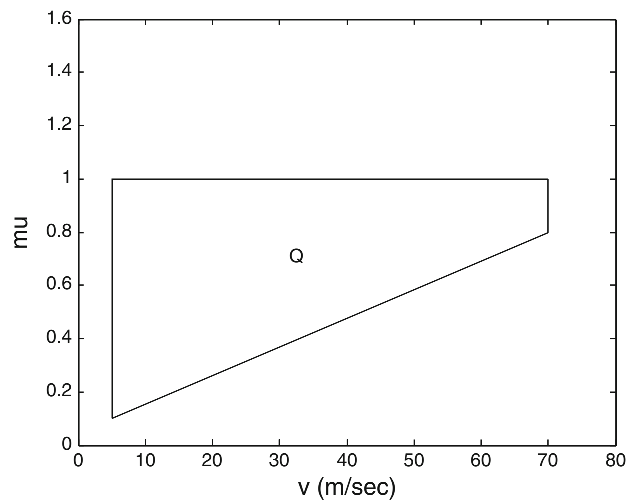

Fig. 4 Operating range

The operating range Q of the uncertain parameters μ and v is depicted in Fig. 4. In addition, the steering actuator is modeled as

$$G_A(s) = \frac{\omega_n^2}{s^2 + \sqrt{2}\omega_n s + \omega_n^2} \tag{27}$$

where $\omega_n = 4\pi$. The open loop transfer function is defined as

$$G_o(s,\mu,v) = G_{r/\delta_f}(s,\mu,v)\cdot G_A(s) \tag{28}$$

4 Simulation results

Consider the static neural control system shown in Fig. 5 and Eq. (28), the open loop transfer function can be obtained as

$$G(s,k_p,k_d,k_u,\mu,v) = \frac{k_p + s\cdot k_d}{\sqrt{2}}\cdot\frac{k_u}{s}\cdot G_O(s,\mu,v). \tag{29}$$

Combining with a gain-phase margin tester, $Ke^{-j\theta}$ and a static neural controller, N_1, the closed loop transfer function is

$$\frac{Ke^{-j\theta}N_1 G(s,k_p,k_d,k_u,\mu,v)}{1+Ke^{-j\theta}N_1 G(s,k_p,k_d,k_u,\mu,v)} = 0 \tag{30}$$

Assume the input signal of N_1 is $x(t) = A\sin\omega t$; the describing function of static neural controller can be expressed as Eq. (20). After some manipulations, the characteristic equation of Eq. (30) is

$$f(s,k_p,k_d,k_u,\mu,v) = X\cdot\alpha + Y\cdot\beta + Z = 0 \tag{31}$$

where $\alpha = k_p$ and $\beta = k_d$ are two adjustable parameters and

$$X = Ke^{-j\theta}N_1 k_u(2.1818\times10^{10}\mu v^2 s + 2.2345\times10^{12}\mu^2 v)$$

$$Y = Ke^{-j\theta}N_1 k_u s(2.1818\times10^{10}\mu v^2 s + 2.2345\times10^{12}\mu^2 v)$$

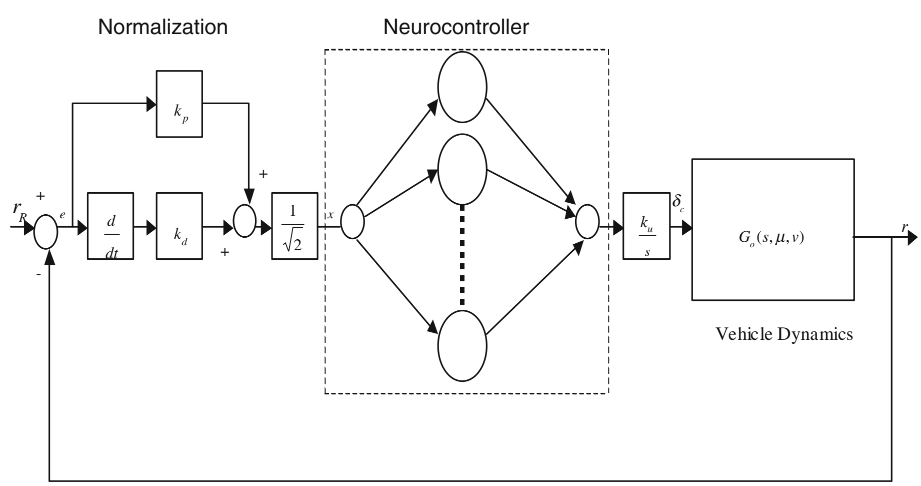

Fig. 5 The block diagram of a neural vehicle control system

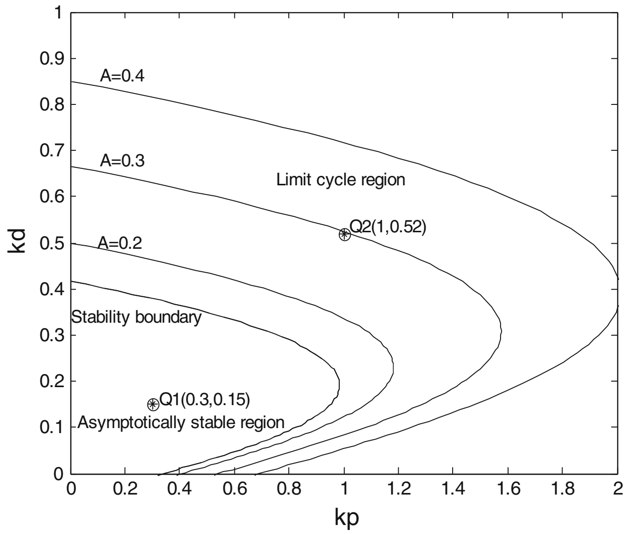

Fig. 6 Limit cycle loci

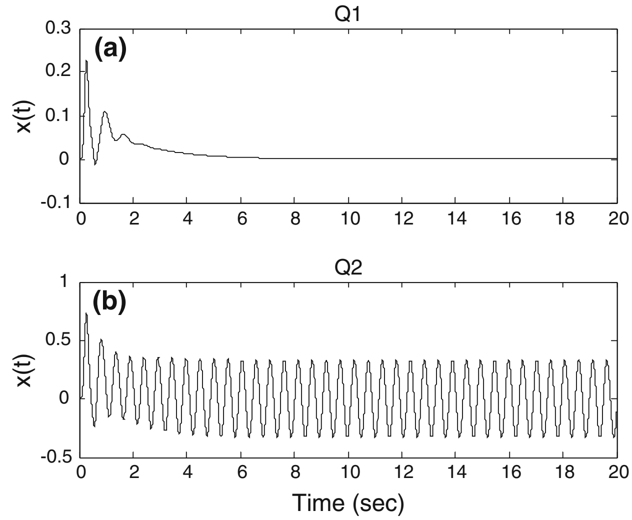

Fig. 7 Input signals $x(t)$

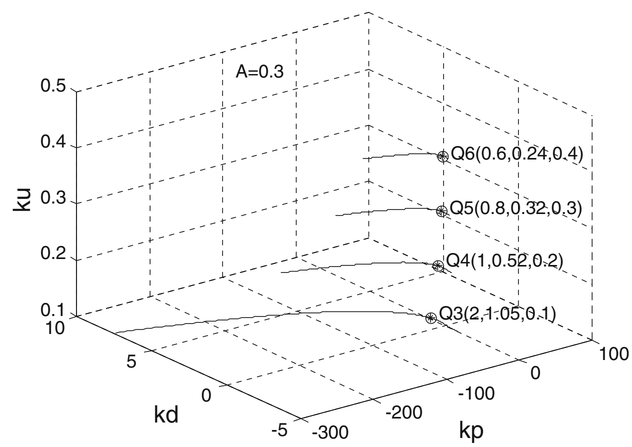

Fig. 8 Limit cycle loci in the parameter space

$$Z = 1.414s(s^2 + 17.7688s + 157.9137)(6.675 \times 10^6 v^2 s^2 + 1.0746 \times 10^9 \mu v s + 4.0045 \times 10^{10} \mu^2 + 1.034 \times 10^8 \mu v^2)$$

Substituting $s = j\omega$ into Eq. (31) enables α and β to be determined from Eqs. (6)–(9) by varying ω from 0 to ∞. Then, the stability boundary ($K = 0$ dB, $\theta = 0°$) can be plotted in the k_p versus k_d plane. Choosing $k_u = 0.2$, $\mu = 1$, $v = 70$ (the highest velocity and road adhesion factor) and the weights g_k and h_k are assumed as follows: $g_1 = g_2 = g_3 = 5$, $h_1 = h_2 = h_3 = 1$.

Then, the describing function N_1 of neural controller can be obtained by using Eq. (20). Figure 6 shows some limit cycle loci. In order to test the accuracy of Fig. 6, two points $Q_1(0.3, 0.15)$ (asymptotically stable region: $A = 0$) and $Q_2(1, 0.52)$ (limit cycle region: $A = 0.3$) are selected. The input signal $x(t)$ shown in Fig. 7 can be obtained by using the famous tool, MATLAB/Simulink. We can clearly find that the amplitude of $x(t)$ operating at two points Q_1 and Q_2 in Fig. 7 is matched with the predicted results in Fig. 6. On the other hand, if k_u is changed from 0.1 to 0.4 and let $A = 0.3$, then the limit cycle loci can be plotted in the $k_p - k_d - k_u$ parameter space. Figure 8 shows the results. Four operating points Q_3–Q_6 are illustrated for testing. The input signals $x(t)$ are obtained in Fig. 9, which consist the results in Fig. 8.

Due to analyzing the gain-phase margins for limit cycle prediction, the operating point Q_1 is chosen. Firstly, let $\theta = 0°$. Equation (31) can be arranged as

$$f(s) = E \cdot K + F = 0 \tag{32}$$

where

$$E = N_1 k_u (k_p + k_d s)(2.1818 \times 10^{10} \mu v^2 s + 2.2345 \times 10^{12} \mu^2 v)$$

$$F = 1.414s(s^2 + 17.7688s + 157.9137)(6.675 \times 10^6 v^2 s^2 + 1.0746 \times 10^9 \mu v s + 4.0045 \times 10^{10} \mu^2 + 1.034 \times 10^8 \mu v^2)$$

By utilizing Eqs. (11)–(14), a set of GM can be obtained and plotted in Fig. 10. If GM = 10 dB is selected, the predicted amplitude of limit cycle is 0.32. In Fig. 11, the input signal $x(t)$ is depicted, and the amplitude of limit cycles conforms to the results in Fig. 10. On the other hand, let $K = 0$dB. Equation (31) can be also arranged as

$$f(s) = U \cdot \cos\theta + V \cdot \sin\theta + W = 0, \tag{33}$$

where

$$U = N_1 k_u (k_p + k_d s)(2.1818 \times 10^{10} \mu v^2 s + 2.2345 \times 10^{12} \mu^2 v)$$

$$V = -jN_1 k_u (k_p + k_d s)(2.1818 \times 10^{10} \mu v^2 s + 2.2345 \times 10^{12} \mu^2 v)$$

Fig. 9 Input signals $x(t)$

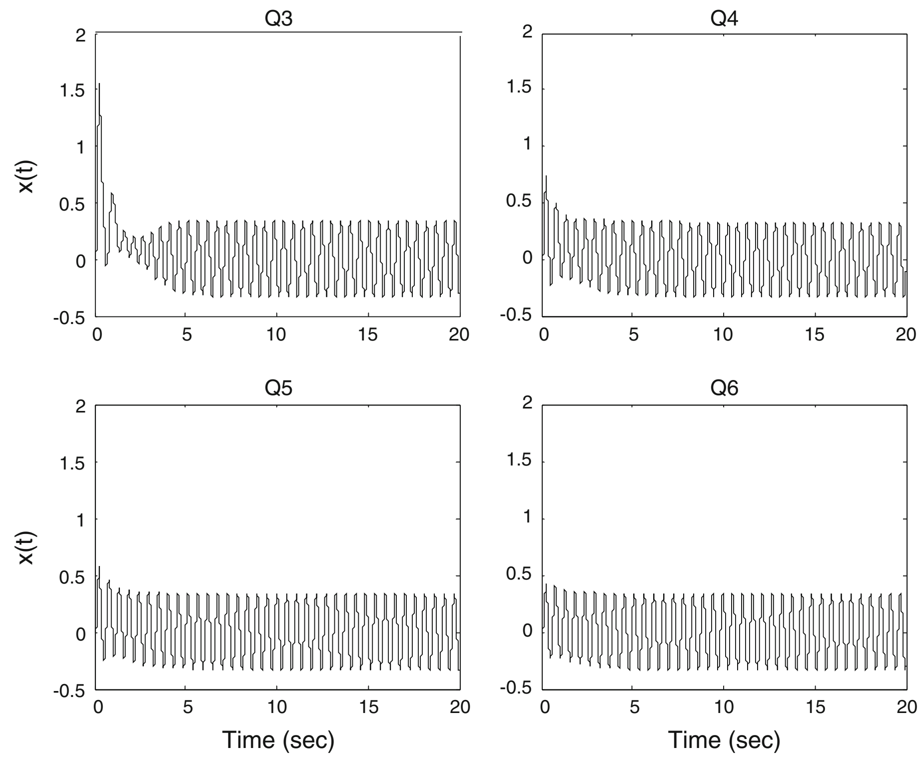

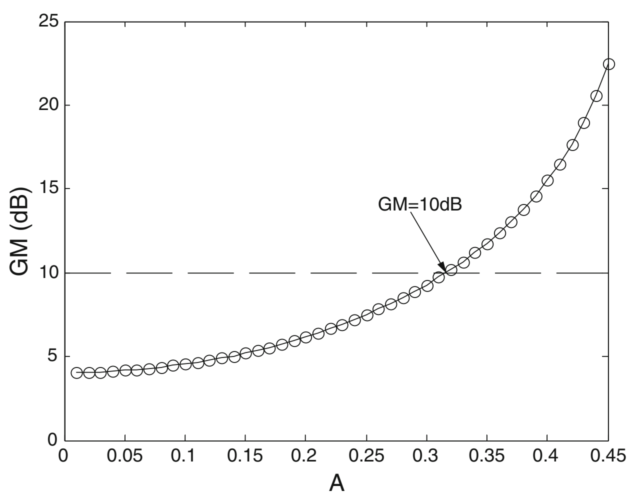

Fig. 10 Gain margin (GM) and amplitude of limit cycle

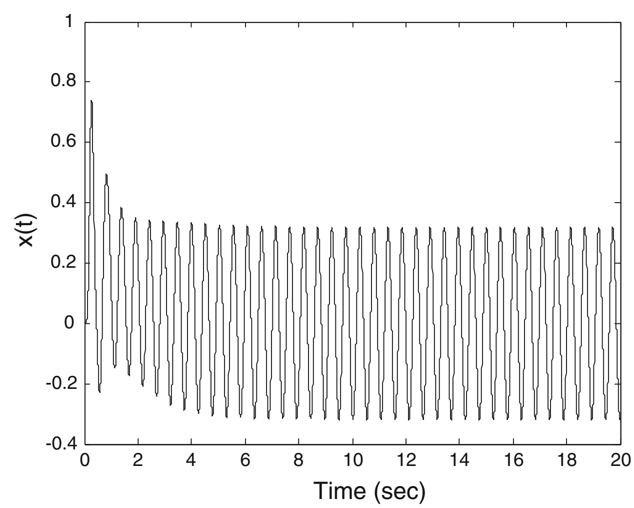

Fig. 11 Input signal $x(t)$

$$W=1.414s(s^2+17.7688s+157.9137)(6.675\times10^6v^2s^2 +1.0746\times10^9\mu vs+4.0045\times10^{10}\mu^2+1.034\times10^8\mu v^2)$$

By utilizing Eqs. (16)–(19), a set of PM can be obtained and plotted in Fig. 12. If PM = 45° is selected, the predicted amplitude of limit cycle is 0.31. In Fig. 13, the input signal $x(t)$ is also depicted and the amplitude of limit cycles conforms to the results in Fig. 12.

Remark 1 The proposed method here can be easily applied to analyze the phenomena of limit cycles even if the control system has multiple nonlinearities, like saturation, relay, hysteresis, backlash and different operating points.

5 Conclusions

In this paper, the limit cycle prediction of a neural vehicle control system with adjustable parameters is achieved by utilizing the frequency domain approaches with describing function, parameter plane and gain-phase margin tester.

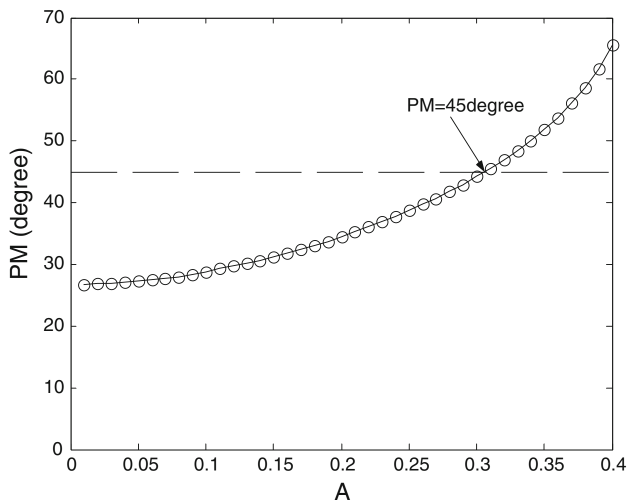

Fig. 12 Phase margin (PM) and amplitude of limit cycle

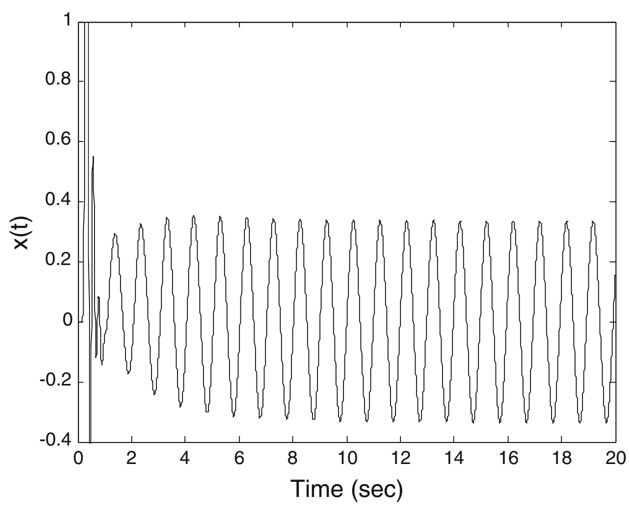

Fig. 13 Input signal $x(t)$

In addition, a simple method is also proposed to point out the gain margin and phase margin when limit cycles can occur in an operating point. A single track vehicle model is then illustrated to study. Finally, computer simulations show that more information about the characteristics of limit cycles could be acquired by this work.

References

1. Gelb A, Velde WEV (1968) Multiple input describing functions and nonlinear system design. McGraw-Hill, New York
2. Siljak DD (1969) Nonlinear systems—the parameter analysis and design. Wiley, New York
3. Han KW (1977) Nonlinear control systems—some practical methods. Academic Cultural Company, California
4. Miller RK, Michel AN, Krenz GS (1983) On the stability of limit cycles in nonlinear feedback systems: analysis using describing functions. IEEE Trans Circuits Syst CAS-30(9):684–696
5. Krenz GS, Miller RK (1986) Qualitative analysis of oscillations in nonlinear control Systems: a describing function approach. IEEE Trans Circuits Syst CAS-33(5):562–566
6. Chung SC, Huang SR, Huang JS, Lee EC (2001) Applications of describing functions to estimate the performance of nonlinear inductance. IEE Proc Sci Meas Technol 148(3):108–114
7. Amato F, Iervolino R, Scala S, Verde L (2001) Category II pilot in–the-loop oscillations analysis from robust stability methods. J Guid Control Dyn 24(3):531–538
8. Wang QG, Zou B, Lee TH, Bi Q (1997) Auto-tuning of multi-variable PID controllers from decentralized relay feedback. Automatica 33(3):319–330
9. Ackermann J, Bunte T (1997) Actuator rate limits in robust car steering control. In: Proceedings of the IEEE conference on decision and control, pp 4726–4731
10. Gordillo F, Aracil J, Alamo T (1997) Determining limit cycles in fuzzy control systems. In: Proceedings of the IEEE international conference on fuzzy systems, pp 193–198
11. Kim E, Lee H, Park M (2000) Limit-cycle prediction of a fuzzy control system based on describing function method. IEEE Trans Fuzzy Syst 8(1):11–21
12. Delgado A (1998) Stability analysis of neurocontrol systems using a describing function. In: Proceedings of the international joint conference on neural networks, pp 2126–2130
13. Delgado A, Warwick K, Kambhampati C (1998) Limit cycles in neurocontrolled minirobots. In: Proceedings of the UKACC international conference control, pp 173–177
14. Siljak DD (1989) Parameter space methods for robust control design: a guide tour. IEEE Trans Automat Contr 34(7):674–688
15. Han KW, Thaler GJ (1966) Control system analysis and design using a parameter space method. IEEE Trans Automat Contr 11(3):560–563
16. Ackermann J (1980) Parameter space design of robust control systems. IEEE Trans Automat Contr 25(6):1058–1072
17. Cavallo A, Maria GE, Verde L (1992) Robust control systems: a parameter space design. J Guid Control Dyn 15(5):1207–1215
18. Chang CH, Han KW (1990) Gain margins and phase margins for control systems with adjustable parameters. J Guid Control Dyn 13(3):404–408
19. Chang CH, Han KW (1989) Gain margin and phase margin analysis of a nuclear reactor control system with multiple transport lags. IEEE Trans Nucl Sci 36(4):1418–1425
20. Shenton AT, Shafiei Z (1994) Relative stability for control systems with adjustable parameters. J Guid Control Dyn 17(2):304–310
21. Chang CH, Chang MK (1994) Analysis of gain margins and phase margins of a nonlinear reactor control system. IEEE Trans Nucl Sci 41(4):1686–1691
22. Chang MK, Chang CH, Han KW (1993) Gain margins and phase margins for nonlinear control systems with adjustable parameters. In: Proceedings of the IEEE transaction industry and application society conference, pp 2123–2130
23. Chang YC, Han KW (1998) Analysis of limit cycles for a low flying vehicle with three nonlinearities. J Actual Probl Aviat Aerosp Syst 6(2):38–50
24. Wu BF, Perng JW, Chin HI (2005) Limit cycle analysis of nonlinear sampled-data systems by gain-phase margin approach. J Franklin Inst 342(2):175–192